

Cueless EEG imagined speech for subject identification: dataset and benchmarks

Ali Derakhshesh¹, Zahra Dehghanian¹, Reza Ebrahimpour², and Hamid R. Rabiee^{1,*}

¹Department of Computer Engineering, Sharif University of Technology, Tehran, Iran

²Center for Cognitive Science, Institute for Convergence Science and Technology (ICST), Sharif University of Technology, Tehran, Iran

*corresponding author(s): Hamid R. Rabiee (rabiee@sharif.edu)

ABSTRACT

Electroencephalogram (EEG) signals have emerged as a promising modality for biometric identification. While previous studies have explored the use of imagined speech with semantically meaningful words for subject identification, most have relied on additional visual or auditory cues. In this study, we introduce a cueless EEG-based imagined speech paradigm, where subjects imagine the pronunciation of semantically meaningful words without any external cues. This innovative approach addresses the limitations of prior methods by requiring subjects to select and imagine words from a predefined list naturally. The dataset comprises over 4,350 trials from 11 subjects across five sessions. We assess a variety of classification methods, including traditional machine learning techniques such as Support Vector Machines (SVM) and XGBoost, as well as time-series foundation models and deep learning architectures specifically designed for EEG classification, such as EEG Conformer and Shallow ConvNet. A session-based hold-out validation strategy was employed to ensure reliable evaluation and prevent data leakage. Our results demonstrate outstanding classification accuracy, reaching 97.93%. These findings highlight the potential of cueless EEG paradigms for secure and reliable subject identification in real-world applications, such as brain-computer interfaces (BCIs).

1. Introduction

A biometric security system could be developed using the integration of biometric databases with recognition techniques. This system works by capturing biometric information from individuals, extracting a set of discriminative features, and matching these features against pre-stored templates within the biometric database.¹ A significant number of researchers employ machine learning or deep learning models as the aforementioned recognition techniques, utilizing datasets composed of biometric samples from individuals. These systems could be developed using two distinct approaches: subject identification and subject authentication, which Bidgoly et al.² clearly distinguished. In subject identification, each individual is treated as a separate class, and the model performs multi-class classification to assign the input to one of these classes. On the other hand, in subject authentication, the model functions as a binary classifier to either accept or deny the claimed identity of the input.

In biometric subject recognition literature, various types of biometric data have been utilized. For instance, Grosz et al.³ used fingerprint data and developed a deep learning architecture named AFR-Net for both subject identification and authentication. Alay et al.⁴ utilized multimodal biometrics, including iris, face, and finger vein data, and implemented a CNN-based model for subject identification. Additionally, other studies have investigated the use of palmprints⁵ and ECG signals⁶ for subject identification.

An electroencephalogram (EEG) is a bioelectric signal generated by neural processes in the brain, carrying extensive information about the brain activity. The acquisition methods of EEG are classified into surface EEG and deep EEG. Surface EEG refers to the use of electrodes on the scalp to record the brain's electrical activity.⁷ In this work, when we refer to EEG, we specifically mean surface EEG. The signal recorded by EEG has poor spatial resolution and a low signal-to-noise ratio; however, due to its safety and high temporal resolution in capturing neural signals' dynamic changes, it remains popular among researchers.⁸

EEG has attracted significant interest as a biometric for subject identification due to its unique advantages. Unlike fingerprints, which can be forged or spoofed, EEG is difficult to replicate. In coercive situations, EEG patterns change, allowing systems to detect if a subject is under duress. Furthermore, EEG ensures the presence of a living subject, as a dead body cannot produce EEG signals.²

Here, we design a cueless EEG imagined speech paradigm and provide a dataset based on this paradigm, which includes multiple sessions for each subject. We then implement a classification framework to identify subjects from this dataset using both machine learning and deep learning approaches.

These findings make three key contributions: (1) introducing a more naturalistic cueless paradigm for EEG data collection, (2) providing a new high-quality dataset for the research community, and (3) establishing comprehensive benchmarks using current state-of-the-art methods.

II. Related works

Researchers have employed various EEG-based paradigms for identifying subjects through brain signals. Some have employed the resting-state EEG paradigm, with eyes-closed and eyes-open conditions, similar to the work of Di et al.⁹. Another commonly used paradigm is motor imagery, where Das et al.¹⁰ identified subjects based on EEG signals recorded during imagined movements of the right arm, left arm, right leg, and left leg. Additionally, other paradigms, such as steady-state visual evoked potentials (SSVEPs)¹¹ and eye blinking¹², have also been explored for subject identification.

Imagined speech as a speech-related paradigm has also been utilized for subject identification. Nieto et al.¹³ distinguished various speech-related paradigms and defined imagined speech as the motor imagery of speaking, where participants are required to feel as though they are producing speech focusing on the mental simulation of articulatory gestures without any actual physical movements.

Brigham et al.¹⁴ explored imagined speech for subject identification using the syllables /ba/ and /ku/. However, Moctezuma et al.¹ raised concerns about this approach for not incorporating words with semantic meaning and subsequently introduced a new dataset featuring the imagined words "up," "down," "left," "right," and "select" in Spanish. In their study, they employed a random forest classifier on discrete wavelet transform energy coefficients to identify subjects. Despite their contributions, their model evaluation approach has limitations, as they used 10-fold cross-validation, which involves shuffling the data. Since their dataset contains only one session per subject, shuffling results in training and test samples being drawn from the same session failing to demonstrate the model’s robustness across sessions over time.

Furthermore, several other datasets containing imagined speech of words with semantic meanings are available, as summarized in Table 1.

Table 1. EEG-based imagined speech datasets featuring words with semantic meanings.

Dataset	Language	Cue Type	Target Words / Commands
Coretto et al. ¹⁵	Spanish	Visual + Auditory	up, down, right, left, forward, backward
Asghari Bejestani et al. ¹⁶	Persian	Auditory	up, down, left, right, yes, no
Qureshi et al. ¹⁷	English	Auditory	go, back, left, right, stop
BCI Competition 2020 Track3 ¹⁸	English	Auditory	hello, help me, stop, yes, thank you

While these studies provide valuable EEG-based datasets in imagined speech paradigms, our investigation reveals that they all rely on visual or auditory cues during the data collection procedure. This setup directs the subject to simulate the target (word or command) corresponding to the presented visual or auditory cue in each trial. However, this method contrasts with real-world scenarios, where a subject would naturally simulate a command of their choice without any additional visual or auditory cues, and these cues may affect the validity of pure imagined speech based subject identification studies.

To address these gaps, our study introduces an imagined speech paradigm for subject identification that eliminates the use of visual or auditory cues. In each trial, subjects naturally select and imagine the pronunciation of a word from a predefined list of five words without being visually or auditorily presented with the words during the trial. This approach ensures that the imagined speech process is more aligned with real-world scenarios. Our dataset consists of over 4,350 trials collected from eleven subjects, spanning five sessions per subject conducted within a single day. This allows us to explore the robustness of models over time. Additionally, we adopt a valid evaluation methodology, ensuring that training and testing samples are drawn from different sessions causally, demonstrating the model’s ability to generalize across temporal variations.

A comparison between our dataset and those from other EEG datasets with the imagined speech task is presented in Table 2.

III. METHODS AND MATERIALS

A. PARTICIPANTS

Eleven healthy participants, all right-handed native Persian speakers with no history of neurological issues, voluntarily participated in this experiment and provided written informed consent. The group consists of 7 males and 4 females, aged between 21 and 28 years, with a mean age of 23.82 years (std = ±2.44). The participants engaged in approximately three hours of recording. In this study, participants are identified by IDs ranging from “Sub-01” to “Sub-11”. Details about each of them are provided in Table 3.

Table 2. Comparison of different EEG-based imagined speech datasets based on being cueless and using semantically meaningful words.

Dataset	Cueless	Semantic words
Zhao et al. (KARA ONE) ¹⁹	×	×
Brigham et al. ¹⁴	✓	×
Moctezuma et al. ¹	×	✓
Coretto et al. ¹⁵	×	✓
Asghari Bejestani et al. ¹⁶	×	✓
Qureshi et al. ¹⁷	×	✓
BCI Competition 2020 Track3 ¹⁸	×	✓
Our Study	✓	✓

Table 3. Participants information.

Subject ID	Sub-01	Sub-02	Sub-03	Sub-04	Sub-05	Sub-06	Sub-07	Sub-08	Sub-09	Sub-10	Sub-11
Gender	Male	Male	Male	Male	Male	Male	Male	Female	Female	Female	Female
Age	23	24	22	24	21	21	24	27	28	21	27

B. EXPERIMENTAL PROTOCOL

During the recording sessions, subjects sat comfortably in an armchair about 60 centimeters from an LCD, which was only used to signal when they should imagine the pronunciation, in a dark, silent room. To capture intra-subject variance, data was collected in five sessions on the same day for each subject. This approach can help researchers design identification systems that are more robust to intra-subject distribution shifts. The necessary instructions were provided during the installation of the EEG cap and electrodes on the subject’s head.

Since the subjects are native Persian speakers, five Persian words were selected as targets. These words correspond to "Left," "Right," "Forward," "Backward," and "Stop" in English. Information about the pronunciation and the corresponding English equivalent of each word is provided in Table 4.

Table 4. Words IPA (International Phonetic Alphabet) pronunciations in Persian and their corresponding English equivalents.

Word Pronunciation in Persian (IPA)	English Equivalent
/tʃæp/	Left
/rɑːst/	Right
/dʒelo/	Forward
/æyæb/	Backward
/ist/	Stop

The experiment paradigm was developed using PsychoPy²⁰ software. At the start of each session, a welcome message displaying the list of words is shown on the screen for 10 seconds. We emphasize that this message is shown only at the beginning of each session, not before each trial. The subject independently selects one of the words from the list before pressing the "space" button on the keyboard to begin each trial. Since movements can affect EEG signals, fixation intervals are used to minimize this. After pressing the "space" button, the subject must avoid moving any body parts, including hands. A gray circle will then appear on the screen for a random duration, uniformly distributed between 1 and 2 seconds. This gap allows the subject to stabilize, ensuring that any hand movement artifacts from pressing the keyboard do not interfere with the EEG signals during the imagined speech phase in the upcoming part. This method helps minimize noise in the EEG data, making the recording more accurate. Afterward, the circle turns blue, indicating that the subject should imagine the pronunciation of the chosen word. The subject imagines the pronunciation once, keeping their eyes open while looking at a blank black screen. The imagination begins as soon as the subject notices the color change to blue, and the blue circle remains on the screen for 2 seconds. Next, the circle turns gray again and remains for 1 second before disappearing. The subject then sees a message on the screen instructing them to select the imagined word by pressing a specific key on the keyboard: 0 key for "Stop", the left arrow key for "Left", the right arrow key for "Right", the up arrow key for "Forward", and the down arrow key for "Backward". If any issues occurred during the 2 second imagination phase, such as unintended movements, imagining multiple words, or an incorrect imagined pronunciation, subject could press the return/enter key to mark the trial as a bad trial for removal in future processing. The trial paradigm, along with the corresponding timings, is also illustrated in Figure 1.

Through several trials and errors in designing the paradigm, the importance of the one-second end fixation became evident. Without it, subjects often began moving their hand to press the key corresponding to the imagined word before the 2-second imagination phase had finished. This early movement introduced artifacts that disturbed the EEG signal during the imagined speech phase. The one-second fixation helps prevent such movement artifacts.

The random 1 to 2 second fixation period before the imagination phase was introduced to prevent the subject from predicting the task. This variability keeps the subject focused and prepared for the upcoming task, while the gap also ensures a reduction in the likelihood of movement artifacts that could disturb the EEG signal.

Each subject participated in 5 sessions, with 100 trials in the first three sessions and 50 in the fourth and fifth sessions. Number of trials in the last two sessions was reduced to minimize the fatigue, which can negatively impact the quality of the EEG signals. The non-fixed trial times allow subjects to take short breaks when needed, helping to prevent fatigue during each session and maintain the quality of their EEG data. Additionally, rest intervals were provided between sessions, during which subjects could drink water and the room lights were turned on to reduce eye strain.

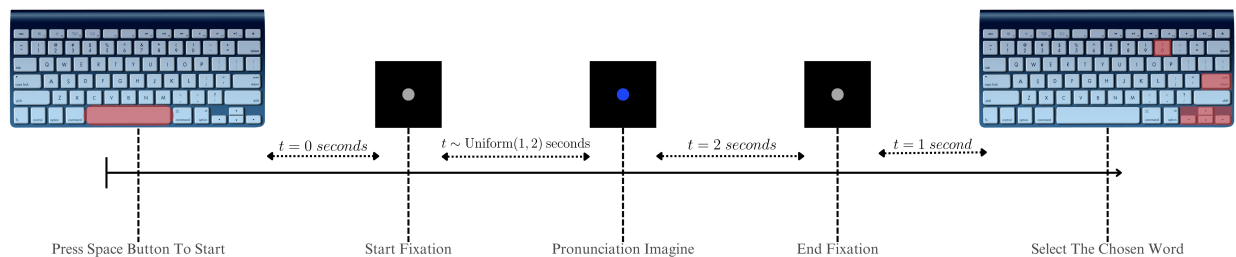


Figure 1. Trial paradigm. Times above the arrow shows the intervals between each phase. Red highlighted buttons on keyboard shows the buttons which subject could press.

C. DATA ACQUISITION

An active EEG device from Liv Intelligent Technology was used for data acquisition (<https://www.livivv.com/en/product>). It includes EEG caps in various sizes, with electrodes positioned according to the 10-20 system²¹. We used the device in this setup, which includes 30 EEG electrodes, one reference electrode, and two ground electrodes which are placed on the left and right earlobes. The EEG channels used in this study are illustrated in Figure 2. The sampling rate was set to 250Hz. For each subject, we used the appropriate size cap. To position the cap on the subject's head, the midpoint between the nasion and inion was identified, and the Cz channel was aligned with this central point. One useful feature of this EEG device is that each EEG electrode is equipped with an LED indicator. The LED glows red when there is no proper contact with the scalp and turns blue once the electrode establishes good contact. Conductive gel was applied to each electrode to ensure proper contact and signal quality. For each session, data from the EEG device is stored in a .tdms file, while the imagined word in each trial is stored in a .csv file.

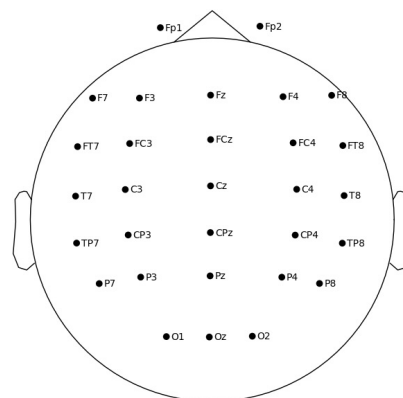


Figure 2. EEG channels used in the experiment, arranged according to the 10-20 system.

D. PRE-PROCESS

To improve the data structure and make information extraction easier for researchers, several pre-processing steps were applied. The pre-processing was performed in Python 3.10.13, primarily using the MNE library²². The Python script for this part is available in the "signal_preprocessing.py" file. Additionally, the raw device output data has been anonymized and is provided alongside the processed data, allowing researchers to adjust or modify the processing steps if needed in the future.

Data structuring and file integration.

As previously mentioned, for each session, a .tdms file containing EEG data and a .csv file with the corresponding words are stored. The .tdms output file is not well-structured and includes only raw triggers indicating when the subject imagined the word. We developed a Python script to integrate the .tdms and .csv files for each session. Using MNE, we annotated the events within the data and removed trials where the subject pressed the return/enter key. Finally, the results were saved in a more organized .fif format. The relevant code for this step can be found in the "data_structuring_file_integration.py" file.

Signal pre-processing.

Pre-processing includes several key techniques to enhance the signal quality, such as applying filters to remove noise, identifying and correcting bad channels, and re-referencing the data. These steps could be done to ensure the EEG recordings are properly cleaned and prepared for further analysis.

- **Notch filter**

Researchers commonly use a Notch filter to remove power line noise, as seen in studies such as Nguyen et al.²³ and Rusnac et al.²⁴. In this study, an overlap-add FIR (Finite Impulse Response) Notch filter was applied using the `notch_filter` function from MNE to remove 50 Hz line noise, as well as its harmonics (e.g., 100 Hz), considering the Nyquist frequency for a sampling rate of 250 Hz.

- **Bandpass filter**

To enhance the signal-to-noise ratio in this study, a FIR bandpass filter with a frequency range of 3 to 45 Hz was applied to the data. The filter utilized a Hamming window, with transition bandwidths of 2 Hz for both the low and high ends.

- **Detect and interpolate bad channels**

Bad channels are those with a low signal-to-noise ratio²⁵. This typically occurs due to poor electrode contact with the scalp. To keep this preprocessing pipeline fully automated and eliminate the need for manual detection of bad channels, we employed the `find_bad_by_correlation` function from the `pyprep` library^{25,26}. In our setup using this function, the data is divided into non-overlapping 1-second windows, and the absolute correlation between each channel and all others is calculated for each window. A window is flagged as bad if its maximum correlation with another channel falls below the threshold of 0.4. Finally, a channel is then marked as bad if the proportion of bad windows exceeds the threshold of 0.02. To maintain data dimensionality across sessions and subjects, bad channels were interpolated rather than being completely removed. We used spherical splines for this interpolation, following the method by Perrin et al.²⁷. For implementation, we utilized the `interpolate_bads` function from MNE, which applies this interpolation method.

- **Re-referencing**

The common average reference removes the common information recorded across electrodes at the same time, which improves the signal-to-noise ratio¹. We applied this method using the `set_eeg_reference` function from MNE, with the `ref_channels` parameter set to average.

IV. Classification Framework

To Show the validity and evaluate our dataset and also establish comprehensive benchmarks, we investigated two distinct approaches for subject identification using pre-processed EEG signals. The first approach follows a two-stage pipeline where features are first extracted from the signals and then fed into classifiers. The second approach uses end-to-end deep learning architectures, specifically designed for EEG classification, that learn both feature representations and classification boundaries directly from the EEG signals to identify the subjects. These approaches are detailed in the following sections.

A. Two-Stage Classification Approaches

Feature extraction followed by shallow classifiers is an established approach in EEG-based subject identification. In this work, we employ two methods for feature extraction. The first method involves manual extraction of domain-specific features from the preprocessed EEG signals, utilizing statistical and signal processing techniques. The second method leverages deep feature extraction, where we fine-tune a foundational time-series deep learning model to extract embeddings from the preprocessed

EEG signals. These extracted features are then fed into shallow classification algorithms, which are trained to distinguish between subjects based on the computed features.

For shallow classification, we utilized two machine learning models: Support Vector Machine (SVM) with a radial basis function (RBF) kernel^{28,29} and XGBoost³⁰ to classify subjects based on the extracted features. These classifiers were chosen to evaluate the effectiveness of extracted features for subject identification in this dataset.

Manual Feature Extraction

We computed two categories of features from the EEG signals: statistical-based and wavelet-based features. For statistical features, we extracted a set of time-domain characteristics including mean, variance, skewness, and kurtosis for each EEG channel. These features capture the statistical properties of the signal's amplitude distribution over time. For wavelet-based features, we computed the energy of wavelet decomposition coefficients for each EEG channel. This approach captures both temporal and spectral characteristics of the signal, providing a suitable representation of the EEG dynamics.

Deep Feature Extraction

For this method, we explored the use of time-series foundation models to extract embeddings directly from EEG signals, rather than relying on handcrafted features. We utilized the MOMENT³¹ model, a transformer-based architecture, and fine-tuned it on our pre-processed dataset to derive meaningful embeddings. These embeddings are designed to capture distinctive characteristics of the EEG signals, enabling effective discrimination between subjects within the embedding space.

MOMENT

MOMENT is a transformer-based model pre-trained on a large collection of public time-series data using a masked prediction method. This self-supervised learning task involves masking portions of the input data and training the model to accurately reconstruct the missing parts. By leveraging this technique, Moment captures intrinsic patterns and characteristics of time-series data.

The authors of MOMENT pre-trained the model using three different architectures for the encoder: T5-Small, T5-Base, and T5-Large. This results in MOMENT having three distinct configurations: the Small model with an embedding dimension of 512, the Base model with an embedding dimension of 768, and the Large model with an embedding dimension of 1024.

The pre-training approach allows Moment to generalize across various types of time-series datasets. The authors demonstrated that, even without dataset-specific fine-tuning, Moment can learn distinct and class-specific representations for diverse time-series data across different fields. In our study, we fine-tuned different sizes of Moment on our dataset to adapt the embeddings for subject identification, utilizing its capability to capture distinctive features from EEG signals that are relevant for distinguishing between subjects.

Shallow Classifiers

For classification using the extracted features, we employed two established machine learning algorithms SVM and XGBoost. These algorithms, often referred to as shallow classifiers to distinguish them from deep learning approaches, have demonstrated strong performance in EEG classification tasks^{32,33}. SVM excels in high-dimensional feature spaces and can effectively handle non-linear relationships through kernel functions, while XGBoost provides robust performance through ensemble learning of decision trees.

SVM is a supervised learning algorithm which aims to find the optimal hyperplane that maximizes the margin between two classes in the feature space. Given the training data $\{(x_1, y_1), \dots, (x_n, y_n)\}$ SVM solves the following optimization problem :

$$\min_{w,b} = \frac{1}{2} \|w\|^2 \text{ subject to } y_i(w^T x_i - b) \geq 1, \forall i \quad (1)$$

where w is the weight vector, b is the bias term, and y_i are the class labels. Then the decision function to classify the data is :

$$f(x) = \text{sgn}(w^T x - b) \quad (2)$$

SVM could also use a kernel function in cases of non-linearly separable data. In this study the radial basis function (RBF) is used as the kernel which is defined as :

$$K(x, x') = \exp\left(-\frac{\|x - x'\|^2}{2\sigma^2}\right) \quad (3)$$

Our second shallow classifier, XGBoost is an efficient and scalable implementation of gradient boosting based on the work by Friedman³⁴. XGBoost builds an ensemble of weak learners, in this study decision trees, by minimizing the following loss

function :

$$L = \sum_{i=1}^N \ell(y_i, \hat{y}_i) + \sum_{k=1}^K \Omega(f_k) \quad (4)$$

Where $\ell(y_i, \hat{y}_i)$ is the loss function that measures the difference between the predicted output \hat{y}_i and the true output y_i , $\Omega(f_k)$ is the regularization term that penalizes the complexity of the model (i.e., the complexity of each tree f_k), N is the number of training samples and K is the number of decision trees. Finally the prediction for an input instance is given by :

$$\hat{y}_i = \sum_{k=1}^K f_k(x_i), f_k \in F \quad (5)$$

where k is the number of trees, f_k is a function in the functional space F , and F is the set of all possible decision trees.

B. End-to-End Deep Learning Approaches

End-to-end deep learning models have become increasingly popular in EEG signal processing because they can learn optimal feature representations directly from data, eliminating the need for manual feature engineering. This automated feature learning can potentially capture subtle patterns and dependencies in EEG signals that might be overlooked by traditional handcrafted features. Additionally, by jointly optimizing feature extraction and classification, these models can adapt to dataset-specific characteristics and potentially achieve better performance.

Here, we utilized several deep learning architectures that have been specifically introduced for EEG classification and brain-computer interface (BCI) tasks. The models employed include EEGNet³⁵, Shallow ConvNet³⁶ and EEG conformer³⁷. The architecture of these models is designed to automatically capture complex discriminative features of EEG signals with respect to the target classes, allowing for more accurate and efficient subject identification. In our study we applied these models directly to the pre-processed EEG signals to identify subjects.

EEGNet

EEGNet is a compact convolutional neural network (CNN) specifically designed for EEG-based BCIs³⁵. It utilizes separable convolutions, which reduce the number of trainable parameters, making the model more compact without decreasing the performance. EEGNet leverages spatial and temporal convolutions that are applied to EEG signals, which have distinctive frequency and spatial characteristics.

The architecture is structured in two main blocks. Block 1 applies temporal convolutions followed by depthwise spatial convolutions to capture both temporal dynamics and spatial relationships across EEG channels. Block 2 employs separable convolutions to further decrease model complexity while combining the extracted features. The output features are then passed through a softmax classifier to perform the final classification.

Shallow ConvNet

Shallow ConvNet is a CNN architecture inspired by the Filter Bank Common Spatial Patterns (FBCSP) approach introduced by Ang et al.³⁸. Unlike FBCSP, which separates feature extraction and classification into distinct stages, Shallow ConvNet integrates these stages within a single network, allowing the model to learn all transformations jointly. The architecture begins with temporal convolution and spatial filtering layers, similar to the bandpass and common spatial pattern (CSP) steps in FBCSP. Following these transformations, the model applies a squaring nonlinearity, mean pooling, and a logarithmic activation function, which together replicate the log-variance computation performed in the FBCSP pipeline. Additionally the Shallow ConvNet use of multiple pooling regions within a trial allows it to learn the temporal structure of band power changes, which enhances classification performance.

EEG Conformer

EEG Conformer is a novel convolutional transformer architecture which combines convolutional layers with self-attention mechanisms³⁹ to capture both local and global features of EEG signals. Unlike conventional convolutional networks that typically focus on local temporal patterns, EEG Conformer incorporates a self-attention module that enables the model to capture long-range dependencies. The convolution module is responsible for learning low-level temporal and spatial features, while the self-attention module extracts global correlations from these local features, allowing the model to understand complex interdependencies in EEG signals.

V. Results

In this section, we present the results of applying the above methods to the pre-processed EEG signals for the subject identification task. In all approaches, each subject is treated as a separate class. To prevent data leakage and ensure proper

training, validation, and testing, we adopted a session-based hold-out validation strategy. Specifically, we used the first three sessions for training, the fourth session for validation, and the final session for testing. this procedure ensures better robustness over time variations and improves the model’s generalization ability. The results are detailed in the subsequent sections.

A. Identification Based On Feature Extraction

The performance of shallow classifiers, including SVM with an RBF kernel and XGBoost, was evaluated using the feature extraction methods including statistical-based features, wavelet-based features, and embeddings extracted from MOMENT model, all derived from the preprocessed EEG signals. The first two feature sets were extracted using the mne-features library⁴⁰. Also for the implementation of the SVM we used scikit-learn library⁴¹ which in the case of multiclass classification, the library handles it using a one-vs-one scheme. In this scheme, a binary classifier is trained for each pair of classes, and the class predicted by the majority of classifiers is chosen as the final classification. The shallow classifiers have hyperparameters that control their complexity and directly affect their performance. To optimize these hyperparameters, the Optuna⁴² framework was utilized.

To perform subject identification using embeddings extracted by MOMENT, we fully fine-tuned the MOMENT model, including its classifier head, to better adapt it to the task and extract more discriminative embeddings. This fine-tuning process aimed to optimize the model’s parameters so that the embeddings could capture features that are more relevant for distinguishing between subjects. For fine-tuning, we followed the hyperparameters suggested by the authors of the MOMENT model. The convergence of the fine-tuning process was observed after 35, 32, and 51 epochs for the large, base, and small configurations, respectively. To evaluate the performance of shallow classifiers on the embeddings extracted by MOMENT, we also removed the classifier head after fine-tuning. This allowed us to feed the extracted embeddings directly into shallow classifiers to assess their effectiveness in subject identification. The results for shallow models applied on different feature sets, are presented in Table 5. Also the results of subject identification based on zero-shot MOMENT is available in appendix.

Table 5. Performance of subject identification based on applying shallow classifiers to manual extracted features.

Model	Model input	Accuracy(%)	Precision(%)	Recall(%)
RBF SVM	statistical-based features	84.40	85.34	84.45
	wavelet-based features	94.17	94.64	94.16
	MOMENT-small embeddings	89.47	89.78	89.51
	MOMENT-base embeddings	88.72	88.72	88.74
	MOMENT-large embeddings	87.41	87.70	87.42
XGBoost	statistical-based features	77.82	82.16	77.94
	wavelet-based features	80.45	79.93	80.47
	MOMENT-small embeddings	86.09	86.81	86.12
	MOMENT-base embeddings	87.22	87.30	87.21
	MOMENT-large embeddings	82.71	83.18	82.76
head classifier	MOMENT-small embeddings	88.53	88.90	88.56
	MOMENT-base embeddings	87.78	87.77	87.80
	MOMENT-large embeddings	86.65	86.76	86.66

t-SNE⁴³ is also used to plot the extracted features of the test data in a 2-dimensional space in Figure 3. The plot visually demonstrates how different feature sets are distributed for different subjects in the test data, providing insight into the separability and clustering of the data in a lower-dimensional space.

B. End-to-End Subject Identification

In this section, we trained three deep learning architectures EEGNet, Shallow ConvNet, and EEG Conformer directly on the pre-processed EEG signals, which were described in the previous section. To implement these models effectively, we utilized the Braindecode library⁴⁴, which provides optimized and efficient implementations of these deep learning architectures in Python.

For the training process, the hyperparameters recommended by the Braindecode library were adopted for each model. However, the learning rate, weight decay, as well as training batch size, were optimized using the Optuna framework. The validation dataset was employed for this hyperparameter tuning. Furthermore, training was capped at a maximum of 30 epochs, with early stopping implemented based on the validation accuracy. Specifically, training was stopped if there was no improvement in validation accuracy for six consecutive epochs. The results of these models on the test dataset are presented in Table 6.

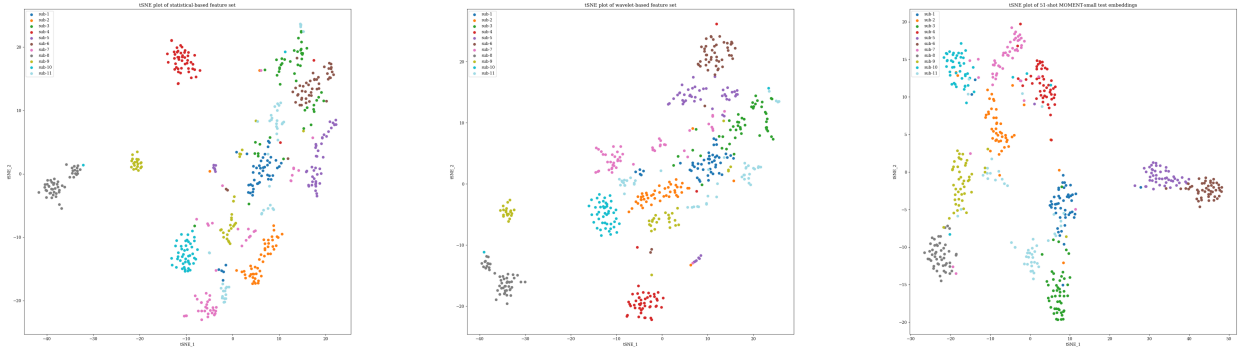


Figure 3. t-SNE visualizations of the extracted features in a 2-dimensional space for subject identification. From left to right, the subplots illustrate statistical features, wavelet features, and fine-tuned MOMENT-small embeddings, respectively.

Table 6. Subject identification results using different end-to-end deep learning models.

Model	Model Input	Accuracy(%)	Precision(%)	Recall(%)
EEGNet	pre-processed EEG	75.56	81.19	75.57
Shallow ConvNet	pre-processed EEG	96.43	96.66	96.43
EEG Conformer	pre-processed EEG	97.93	97.98	97.94

Table 6 shows that Shallow ConvNet and EEG Conformer achieve the highest performance among all the methods evaluated in this study. Consequently, these two models were selected for further analysis to examine the impact of training with fewer sessions. In the subsequent experiment, the models were also trained using two different configurations. One configuration involved training with first two sessions, while the other utilized only the first session (the validation and test data are the same as the other experiments). The result is illustrated in Figure 4.

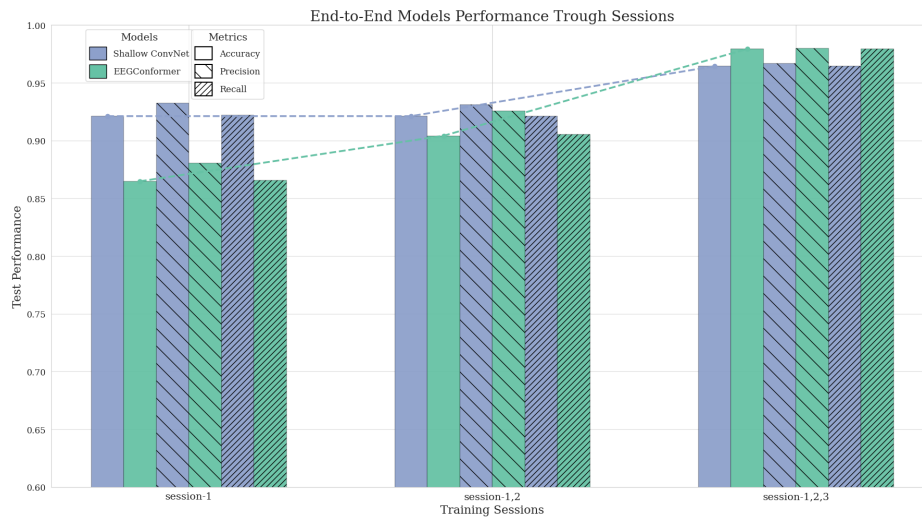


Figure 4. Performance of Shallow ConvNet and EEG Conformer for subject identification using different amount of sessions.

In Figure 4, the x-axis illustrates a decrease in the amount of training data as one moves leftward, along with an increasing time gap between the training and test data. The plot reveals that the performance of the EEG Conformer improves with larger datasets, while its accuracy declines when trained on fewer sessions. In contrast, the Shallow ConvNet maintains more consistent performance even with a reduced number of training sessions. This effect arises because the EEG Conformer integrates a transformer architecture alongside convolutional layers, making it more complex than the Shallow ConvNet model.

Consequently, the EEG Conformer needs a greater volume of training data to achieve optimal performance, whereas the Shallow ConvNet remains effective with smaller datasets. Therefore, for subject identification tasks with limited data, Shallow ConvNet may be more suitable. However, due to the sufficient amount of data in our dataset, EEG Conformer can be utilized to achieve higher performance.

VI. Conclusion

In this study, we introduced a novel cueless EEG paradigm for subject identification, where participants imagine words without external cues. Based on this paradigm, we created a comprehensive dataset containing over 4,350 trials from 11 subjects across multiple sessions. To validate the dataset and establish performance benchmarks, we conducted extensive experiments using a broad spectrum of classification approaches, ranging from traditional feature-based methods to state-of-the-art deep learning architectures. Our evaluation methodology employed session-based hold-out validation, where models were trained and tested on data from different recording sessions. This approach ensures the practical applicability of our results by demonstrating the models ability to generalize across temporal variations. The experimental results demonstrated classification accuracies reaching 97.93%, validating both the quality of our dataset and the effectiveness of modern classification approaches for EEG-based subject identification.

Code Availability

The dataset utilized in this study is publicly accessible at https://huggingface.co/datasets/Alidr79/cueless_EEG_subject_identification. All scripts and code required for data loading, signal processing, training shallow classifiers, fine-tuning MOMENT, and training end-to-end models are available in the GitHub repository at https://github.com/Alidr79/cueless_EEG_subject_identification. The repository includes detailed instructions on how to use it.

References

1. Moctezuma, L. A., Torres-García, A. A., Villaseñor-Pineda, L. & Carrillo, M. Subjects identification using eeg-recorded imagined speech. *Expert. Syst. with Appl.* **118**, 201–208 (2019).
2. Bidgoly, A. J., Bidgoly, H. J. & Arezoumand, Z. A survey on methods and challenges in eeg based authentication. *Comput. & Secur.* **93**, 101788 (2020).
3. Grosz, S. A. & Jain, A. K. Afr-net: Attention-driven fingerprint recognition network. *IEEE Transactions on Biom. Behav. Identity Sci.* (2023).
4. Alay, N. & Al-Baity, H. H. Deep learning approach for multimodal biometric recognition system based on fusion of iris, face, and finger vein traits. *Sensors* **20**, 5523 (2020).
5. Trabelsi, S. *et al.* Efficient palmprint biometric identification systems using deep learning and feature selection methods. *Neural Comput. Appl.* **34**, 12119–12141 (2022).
6. Fatimah, B., Singh, P., Singhal, A. & Pachori, R. B. Biometric identification from ecg signals using fourier decomposition and machine learning. *IEEE Transactions on Instrumentation Meas.* **71**, 1–9 (2022).
7. Qin, Y., Zhang, Y., Zhang, Y., Liu, S. & Guo, X. Application and development of eeg acquisition and feedback technology: A review. *Biosensors* **13**, 930 (2023).
8. Zhang, H. *et al.* The applied principles of eeg analysis methods in neuroscience and clinical neurology. *Mil. Med. Res.* **10**, 67 (2023).
9. Di, Y. *et al.* Robustness analysis of identification using resting-state eeg signals. *Ieee Access* **7**, 42113–42122 (2019).
10. Das, R., Maiorana, E. & Campisi, P. Motor imagery for eeg biometrics using convolutional neural network. In *2018 IEEE international conference on acoustics, speech and signal processing (ICASSP)*, 2062–2066 (IEEE, 2018).
11. Piciuccio, E., Maiorana, E., Falzon, O., Camilleri, K. P. & Campisi, P. Steady-state visual evoked potentials for eeg-based biometric identification. In *2017 International Conference of the Biometrics Special Interest Group (BIOSIG)*, 1–5 (IEEE, 2017).
12. Abo-Zahhad, M., Ahmed, S. M. & Abbas, S. N. A new eeg acquisition protocol for biometric identification using eye blinking signals. *Int. J. Intell. Syst. Appl.* **7**, 48 (2015).
13. Nieto, N., Peterson, V., Rufiner, H. L., Kamienkowski, J. E. & Spies, R. Thinking out loud, an open-access eeg-based bci dataset for inner speech recognition. *Sci. Data* **9**, 52 (2022).

14. Brigham, K. & Kumar, B. V. Subject identification from electroencephalogram (eeg) signals during imagined speech. In *2010 Fourth IEEE International Conference on Biometrics: Theory, Applications and Systems (BTAS)*, 1–8 (IEEE, 2010).
15. Coretto, G. A. P., Gareis, I. E. & Rufiner, H. L. Open access database of eeg signals recorded during imagined speech. In *12th International Symposium on Medical Information Processing and Analysis*, vol. 10160, 1016002 (SPIE, 2017).
16. Asghari Bejestani, M., Mohammad Khani, G. R., Nafisi, V. & Darakeh, F. Eeg-based multiword imagined speech classification for persian words. *BioMed Res. Int.* **2022**, 8333084 (2022).
17. Qureshi, M. N. I. *et al.* Multiclass classification of word imagination speech with hybrid connectivity features. *IEEE Transactions on Biomed. Eng.* **65**, 2168–2177 (2017).
18. Committee, B. C. Bci competition (2020). <https://osf.io/pq7vb/> (Accessed 1 January 2024).
19. Zhao, S. & Rudzicz, F. Classifying phonological categories in imagined and articulated speech. In *2015 IEEE international conference on acoustics, speech and signal processing (ICASSP)*, 992–996 (IEEE, 2015).
20. Peirce, J., Hirst, R. & MacAskill, M. *Building experiments in PsychoPy* (Sage, 2022).
21. Jasper, H. H. Ten-twenty electrode system of the international federation. *Electroencephalogr Clin Neurophysiol* **10**, 371–375 (1958).
22. Gramfort, A. *et al.* Meg and eeg data analysis with mne-python. *Front. Neuroinformatics* **7**, 267 (2013).
23. Nguyen, C. H., Karavas, G. K. & Artemiadis, P. Inferring imagined speech using eeg signals: a new approach using riemannian manifold features. *J. neural engineering* **15**, 016002 (2017).
24. Rusnac, A.-L. & Grigore, O. Imaginary speech recognition using a convolutional network with long-short memory. *Appl. Sci.* **12**, 11873 (2022).
25. Bigdely-Shamlo, N., Mullen, T., Kothe, C., Su, K.-M. & Robbins, K. A. The prep pipeline: standardized preprocessing for large-scale eeg analysis. *Front. neuroinformatics* **9**, 16 (2015).
26. Appelhoff, S. *et al.* PyPREP: A Python implementation of the preprocessing pipeline (PREP) for EEG data., [10.5281/zenodo.10047462](https://doi.org/10.5281/zenodo.10047462) (2023).
27. Perrin, F., Pernier, J., Bertrand, O. & Echallier, J. F. Spherical splines for scalp potential and current density mapping. *Electroencephalogr. clinical neurophysiology* **72**, 184–187 (1989).
28. Cortes, C. Support-vector networks. *Mach. Learn.* (1995).
29. Schölkopf, B. Learning with kernels: support vector machines, regularization, optimization, and beyond (2002).
30. Chen, T. & Guestrin, C. Xgboost: A scalable tree boosting system. In *Proceedings of the 22nd acm sigkdd international conference on knowledge discovery and data mining*, 785–794 (2016).
31. Goswami, M. *et al.* Moment: A family of open time-series foundation models. *arXiv preprint arXiv:2402.03885* (2024).
32. Parui, S., Bajjiya, A. K. R., Samanta, D. & Chakravorty, N. Emotion recognition from eeg signal using xgboost algorithm. In *2019 IEEE 16th India Council International Conference (INDICON)*, 1–4 (IEEE, 2019).
33. Bousseta, R. *et al.* Eeg efficient classification of imagined hand movement using rbf kernel svm. In *2016 11th International Conference on Intelligent Systems: Theories and Applications (SITA)*, 1–6 (IEEE, 2016).
34. Friedman, J. H. Greedy function approximation: a gradient boosting machine. *Annals statistics* 1189–1232 (2001).
35. Lawhern, V. J. *et al.* Eegnet: a compact convolutional neural network for eeg-based brain–computer interfaces. *J. neural engineering* **15**, 056013 (2018).
36. Schirrmester, R. T. *et al.* Deep learning with convolutional neural networks for eeg decoding and visualization. *Hum. brain mapping* **38**, 5391–5420 (2017).
37. Song, Y., Zheng, Q., Liu, B. & Gao, X. Eeg conformer: Convolutional transformer for eeg decoding and visualization. *IEEE Transactions on Neural Syst. Rehabil. Eng.* **31**, 710–719 (2022).
38. Ang, K. K., Chin, Z. Y., Zhang, H. & Guan, C. Filter bank common spatial pattern (fbcspp) in brain-computer interface. In *2008 IEEE international joint conference on neural networks (IEEE world congress on computational intelligence)*, 2390–2397 (IEEE, 2008).
39. Vaswani, A. Attention is all you need. *Adv. Neural Inf. Process. Syst.* (2017).
40. Schiratti, J.-B., Le Douget, J.-E., Le Van Quyen, M., Essid, S. & Gramfort, A. An ensemble learning approach to detect epileptic seizures from long intracranial eeg recordings. In *2018 IEEE International Conference on Acoustics, Speech and Signal Processing (ICASSP)*, 856–860 (IEEE, 2018).

41. Pedregosa, F. *et al.* Scikit-learn: Machine learning in Python. *J. Mach. Learn. Res.* **12**, 2825–2830 (2011).
42. Akiba, T., Sano, S., Yanase, T., Ohta, T. & Koyama, M. Optuna: A next-generation hyperparameter optimization framework. In *Proceedings of the 25th ACM SIGKDD International Conference on Knowledge Discovery and Data Mining* (2019).
43. Van der Maaten, L. & Hinton, G. Visualizing data using t-sne. *J. machine learning research* **9** (2008).
44. Schirrneister, R. T. *et al.* Deep learning with convolutional neural networks for eeg decoding and visualization. *Hum. Brain Mapp.* [10.1002/hbm.23730](https://doi.org/10.1002/hbm.23730) (2017).

Appendix

Zero-shot MOMENT

In this study MOMENT is used in two approaches zero-shot and full fine-tuned to extract features. as MOMENT is pre-trained on time series it can capture some EEG characteristics without fine-tuning. Also all three sizes of MOMENT were tested to compare the performance.

In the zero-shot approach, no fine-tuning is applied to the MOMENT model, and instead, the pre-trained MOMENT is used in inference mode to generate embeddings for each EEG sample. These embeddings, which are extracted without any model adaptation to the specific task, provide a representation of the data that can still be useful for subject identification. The identification results based on zero-shot MOMENT are provided in table 7. In the experiments of this table in addition to shallow classifiers mentioned in previous sections, some experiments are done by fine-tuning the classification head of the MOMENT model keeping all previous layers frozen.

Table 7. Performance of subject identification based on MOMENT zero-shot embeddings

Model	Feature set	Accuracy(%)	Precision(%)	Recall(%)
RBF SVM	MOMENT-large embeddings	79.51	79.91	79.55
XGBoost	MOMENT-large embeddings	78.01	78.46	78.06
RBF SVM	MOMENT-base embeddings	81.39	81.66	81.43
XGBoost	MOMENT-base embeddings	79.14	79.17	79.17
RBF SVM	MOMENT-small embeddings	80.08	80.29	80.13
XGBoost	MOMENT-small embeddings	77.82	78.15	77.86

Visualization of MOMENT Embeddings

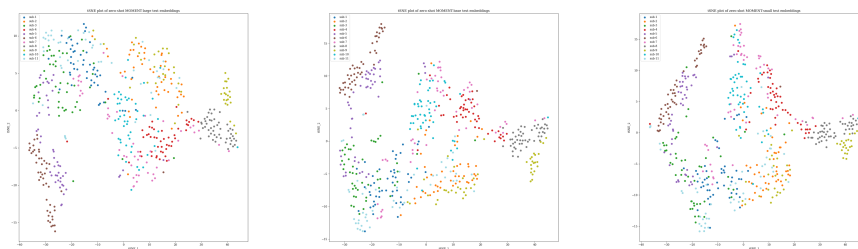


Figure 5. Visualization of zero-shot embeddings for three different MOMENT model sizes: large, base, and small. The embeddings for each model size are shown side-by-side for comparison, highlighting the differences in feature space representation.

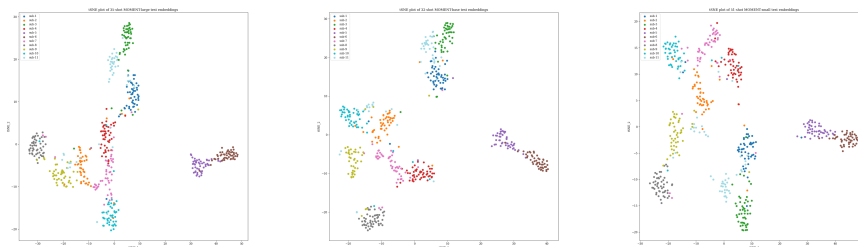


Figure 6. Visualization of fine-tuned embeddings for three different MOMENT model sizes: large, base, and small. The embeddings for each model size are displayed side-by-side for comparison, demonstrating the improvements in feature space separation after fine-tuning.